

# Comparison of $\text{Cl}_2$ and $\text{F}_2$ based chemistries for the inductively coupled plasma etching of NiMnSb thin films

J. Hong, J. A. Caballero, and E. S. Lambers

Department of Materials Science and Engineering, University of Florida, Gainesville, Florida 32611

J. R. Childress

IBM Almaden Research Center, San Jose, California 95120

S. J. Pearton<sup>a)</sup>

Department of Materials Science and Engineering, University of Florida, Gainesville, Florida 32611

(Received 17 August 1998; accepted 1 March 1999)

Plasma etching chemistries based on  $\text{BCl}_3/\text{Ar}$ ,  $\text{BCl}_3/\text{H}_2$  and  $\text{NF}_3/\text{Ar}$  were studied for patterning NiMnSb Heusler alloys thin films and associated  $\text{Al}_2\text{O}_3$  barrier layers in an inductively coupled plasma tool. Using  $\text{BCl}_3/\text{Ar}$  discharges, high etch rates ( $\geq 1 \mu\text{m}/\text{min}$ ) were achieved either at high source power [(1000 W) or high direct current (dc) self bias ( $-300 \text{ V}$ )] and etch rates showed a strong dependence upon source power, ion energy, and gas composition. Hydrogen addition to the  $\text{BCl}_3$  created new species (HCl) in the plasma, leading to faster etch rates for NiMnSb than in the case of Ar addition. Selectivities of  $\geq 8$  for NiMnSb over  $\text{Al}_2\text{O}_3$  were obtained in  $\text{BCl}_3$ -based discharges. On the other hand,  $\text{NF}_3/\text{Ar}$  discharges provided a narrow process window for the etching of NiMnSb and the etch rates were much lower compared to those with  $\text{BCl}_3$ . The surfaces of NiMnSb etched with  $\text{NF}_3/\text{Ar}$  was smoother (root-mean-square surface roughness of 1.4 nm measured by atomic force microscopy) than the surfaces produced with  $\text{BCl}_3/\text{Ar}$ . In terms of near-surface chemistry,  $\text{NF}_3/\text{Ar}$  produced Mn enrichment, indicating the existence of involatile Mn etch products, whereas Mn deficiency was obtained under the same conditions with  $\text{BCl}_3/\text{Ar}$ .

© 1999 American Vacuum Society. [S0734-2101(99)12304-2]

## I. INTRODUCTION

There is a strong development effort underway for magnetic data storage technologies, predominantly magnetic disks and tapes, capable of increased areal storage densities.<sup>1,2</sup> A recent advance has been the introduction of NiFe-based magnetic layer elements based on the giant magnetoresistance effect,<sup>3</sup> leading to the demonstration of areal bit densities  $> 10 \text{ Gbit in}^{-2}$ . It has been suggested that even better control over spin currents in magnetic devices could be achieved in the so-called half-metallic materials.<sup>4</sup> One of the candidates is the Heusler alloy NiMnSb, which has a high Curie temperature (720 K) and can be prepared in thin film form.<sup>5-9</sup> The spin filtering effect of the NiMnSb will be a maximum when the current flow is a normal to the film plane, either resistively or by tunneling through an insulating layer such as  $\text{Al}_2\text{O}_3$ . The development of anisotropic etch processes for these materials are necessary if they are to be implemented in read heads or other magnetic recording or memory applications.

We have previously reported on a comparison of plasma etch chemistries for NiMnSb/ $\text{Al}_2\text{O}_3$  structures under either electron cyclotron resonance (ECR) or inductively coupled plasma (ICP) conditions.<sup>10,11</sup> In ECR tools, selectivities of  $\geq 20$  for NiMnSb over  $\text{Al}_2\text{O}_3$  were obtained in  $\text{SF}_6$  discharges, while selectivities  $\leq 5$  were typical in  $\text{Cl}_2$  and  $\text{BCl}_3$ .<sup>10</sup> In ICP tools, we found that  $\text{SF}_6/\text{Ar}$  discharges produced high etch rates ( $> 1 \mu\text{m min}^{-1}$ ) even at low source

powers, with the same results achieved in ECR tools.<sup>10,11</sup> In this article, we compare the ICP etching characteristics of NiMnSb and  $\text{Al}_2\text{O}_3$  in  $\text{BCl}_3$  and  $\text{NF}_3$  plasma chemistries, in order to better understand the differences between halogen-based chemistries.

## II. EXPERIMENT

5000-Å-thick NiMnSb films were deposited by magnetron sputtering with 30 W rf power at a rate of  $0.6 \text{ \AA s}^{-1}$  onto glass substrates at a temperature of 350 °C.<sup>7</sup>  $\text{Al}_2\text{O}_3$  films were deposited with 140 W rf power ( $0.32 \text{ \AA s}^{-1}$  deposition rate) on Si wafers held at room temperature. The samples were lithographically patterned with AZ5209E photoresist.

The etching was performed in a Plasma Therm 790 system. The plasma is generated in a three turn plasma geometry ICP source (2 MHz, 1500 W). The He backside cooled sample chuck was separately biased with 13.56 MHz power to control ion energy. The process pressure was held constant at 2 mTorr and total gas flow rate was 15 standard cubic centimeters per minute. Two different gas chemistries based on  $\text{Cl}_2$  and  $\text{F}_2$  were investigated with addition of either Ar, in order to provide an enhanced physical component to the etching, or  $\text{H}_2$ , for the effect of new species created.

Etch rates were measured from stylus profilometry of the features after removal of photoresist mask in acetone. The etched surface roughness was examined by atomic force microscopy (AFM) in tapping mode. The near surface chemistry was studied from Auger electron spectroscopy (AES) measurements.

<sup>a)</sup>Electronic mail: spear@mse.ufl.edu

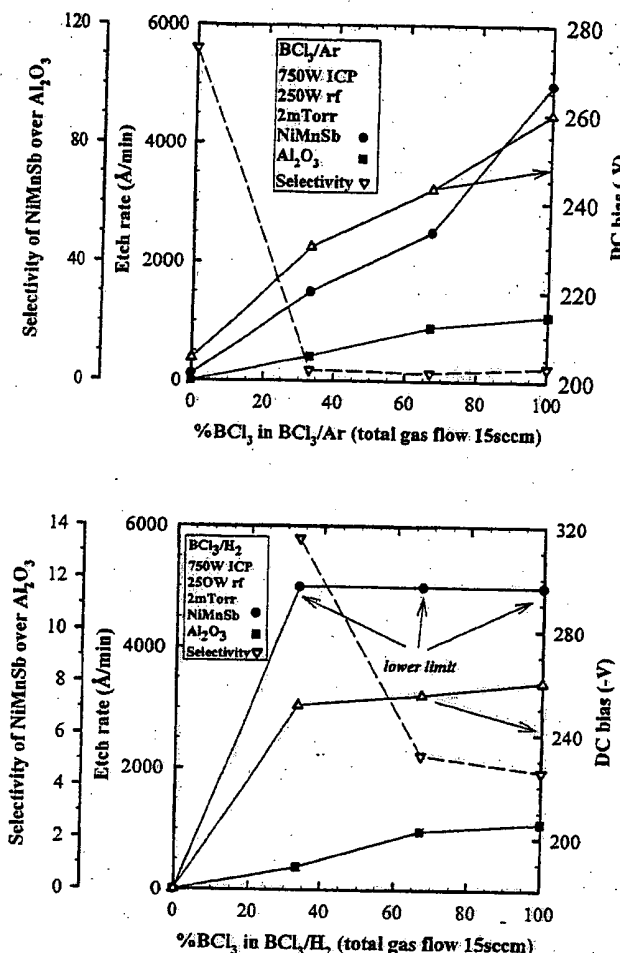


FIG. 1. Etch rates of NiMnSb and Al<sub>2</sub>O<sub>3</sub> and selectivities as a function of plasma composition in 2 mTorr, 750 W ICP, 250 W rf chuck power discharges of either BC<sub>3</sub>/Ar (top) or BC<sub>3</sub>/H<sub>2</sub> (bottom).

### III. RESULTS AND DISCUSSION

Figure 1 shows etch rates of NiMnSb and Al<sub>2</sub>O<sub>3</sub>, and the resulting selectivity, as a function of gas composition in both BC<sub>3</sub>/Ar (top) and BC<sub>3</sub>/H<sub>2</sub> (bottom) discharges. First, direct current (dc) self-bias in both discharges increased with BC<sub>3</sub> concentration which means an increasing chemical component to the etching at higher BC<sub>3</sub> concentration. The removal rate for NiMnSb showed a monotonic increase in the BC<sub>3</sub>/Ar mixture, indicating that the etching at this condition is at least partially reaction limited. Al<sub>2</sub>O<sub>3</sub> showed lower etch rates over the whole range of compositions than NiMnSb, probably due to its higher bond strength (average bond strength 311 kcal mol<sup>-1</sup>, compared to 278 kcal mol<sup>-1</sup>). Selectivity of NiMnSb over Al<sub>2</sub>O<sub>3</sub> was ~5 above 33% BC<sub>3</sub> concentration. By contrast, the BC<sub>3</sub>/H<sub>2</sub> combination provided faster etching of NiMnSb even with small amount (33%) of BC<sub>3</sub>. We ascribe this fact to the creation of new species (HCl) in the plasma, as determined by both mass spectrometry and optical emission spectroscopy. Simple hydride etch products do not appear to be volatile, as evidenced by the low etch rates in pure H<sub>2</sub> plasmas. The HCl appears to

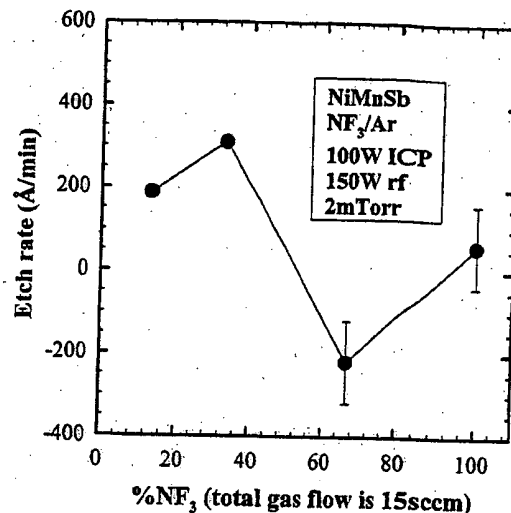


FIG. 2. Etch rate of NiMnSb as a function of NF<sub>3</sub> percentages in 2 mTorr, 100 W ICP, NF<sub>3</sub>/Ar discharges at constant rf chuck power (150 W rf).

provide more efficient etching of the NiMnSb than the Cl neutrals that predominant in BC<sub>3</sub>/Ar discharges. Selectivity achieved at this condition was > 12. We have not yet tried direct etching of NiMnSb with HCl plasmas.

NF<sub>3</sub>/Ar discharges produced somewhat different results. The etch rate of NiMnSb is shown in Fig. 2 as a function of NF<sub>3</sub> percentage. Slow etching occurred up to 33% NF<sub>3</sub> and then reverted to deposition above this composition. The creation of an involatile fluorinated surface at high NF<sub>3</sub> compositions is the cause of these results as described in more detail later.

The etch rates of NiMnSb were also a strong function of source power with the BC<sub>3</sub>/Ar chemistry. As shown in Fig. 3, the etch rate of NiMnSb increased rapidly above 750 W ICP source power even with the suppressed ion energy. The higher ion flux available at high source power and the higher reactive Cl neutral concentration outweighed this ion

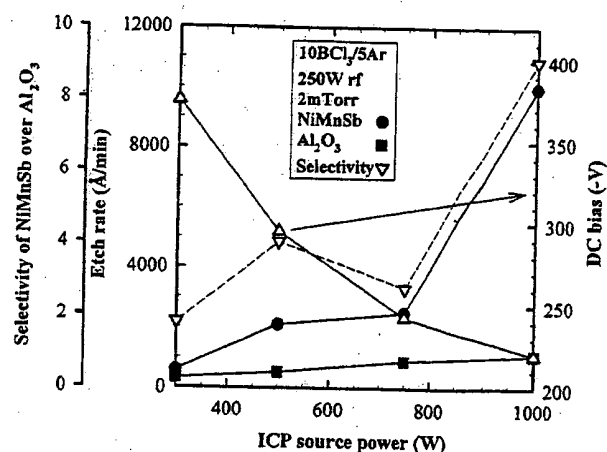


FIG. 3. Etch rates of NiMnSb and Al<sub>2</sub>O<sub>3</sub> and selectivities as a function of ICP source power in 2 mTorr, 250 W rf, 10BC<sub>3</sub>/5Ar discharges.

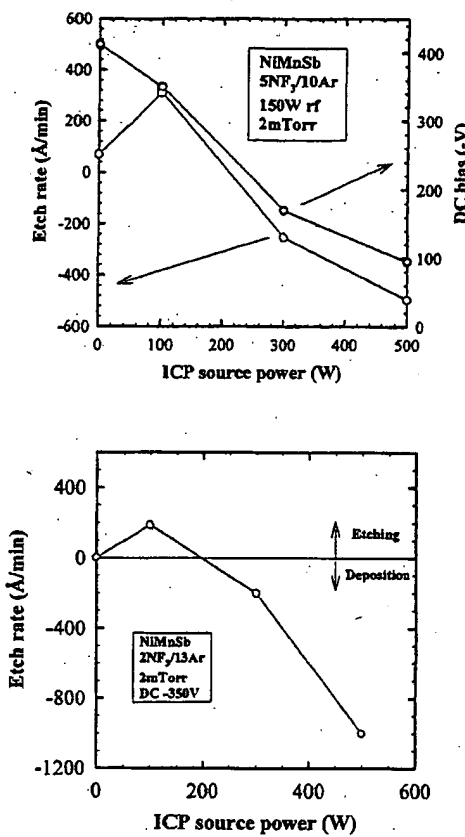


FIG. 4. Etch rate of NiMnSb as a function of ICP source power in either 2 mTorr, 150 W rf, 5NF<sub>3</sub>/10Ar discharges (top) or 2 mTorr, -350 V dc, 2NF<sub>3</sub>/13Ar discharges (bottom).

energy suppression effect. Selectivity achieved at 1000 W source power was >8 since Al<sub>2</sub>O<sub>3</sub> showed consistently slow etching.

We picked up two compositions of the NF<sub>3</sub>/Ar chemistry (5NF<sub>3</sub>/10Ar, 2NF<sub>3</sub>/13Ar) at which etching of NiMnSb occurred. With 5NF<sub>3</sub>/10Ar (Fig. 4, top) at constant radio frequency (rf) chuck power of 150 W, etching proceeded up to

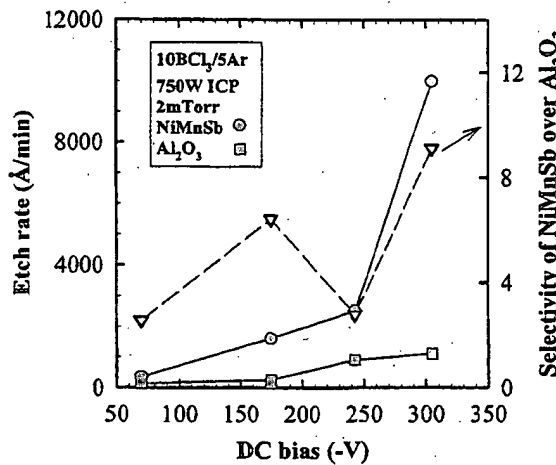


FIG. 5. Etch rates of NiMnSb and Al<sub>2</sub>O<sub>3</sub> and selectivities as a function of dc self-bias in 2 mTorr, 750 W ICP, 10BCl<sub>3</sub>/5Ar discharges.

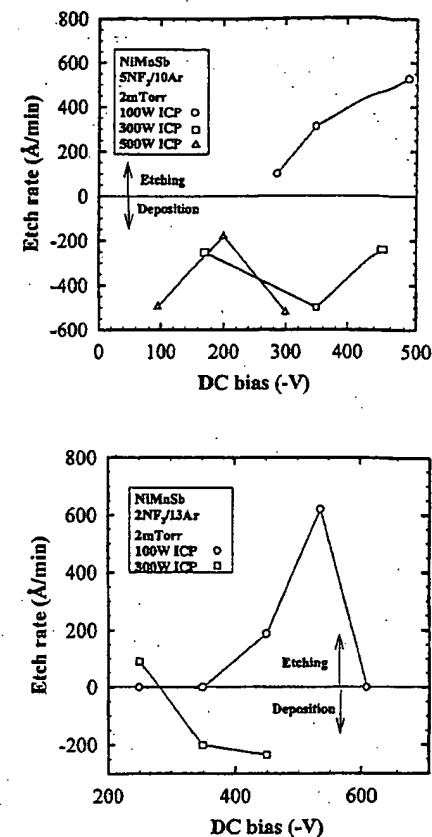


FIG. 6. Etch rate of NiMnSb as a function of dc self bias in either 2 mTorr, 5NF<sub>3</sub>/10Ar discharges (top) or 2 mTorr, 2NF<sub>3</sub>/13Ar discharges (bottom) at different source powers.

100 W ICP source power and then reverted to deposition at higher source powers. We set dc self-bias at constant value of -350 V with 2NF<sub>3</sub>/13Ar (Fig. 4, bottom) to eliminate the effect of ion energy change for the etching. The result obtained was the same as the above case. Etching only occurred

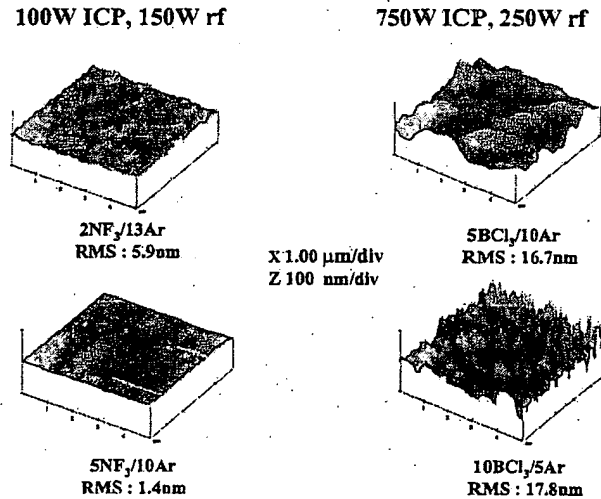


FIG. 7. AFM scans of NiMnSb surfaces after dry etching in different plasma compositions.

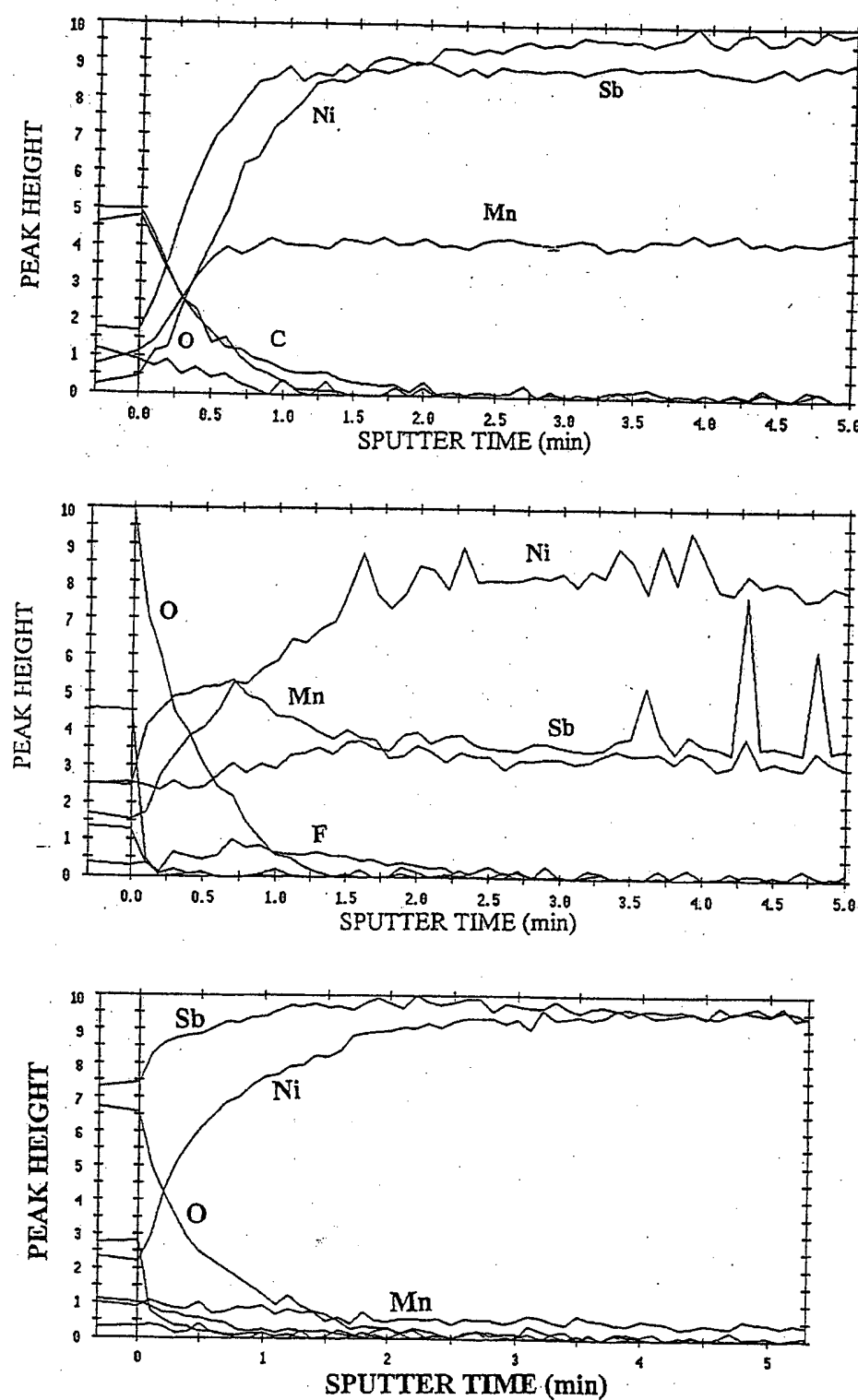


FIG. 8. AES depth profiles of NiMnSb samples before (top), or after ICP etching in either 2 mTorr, 100 W ICP, 150 W rf, 5NF<sub>3</sub>/10Ar discharges (center) or 2 mTorr, 750 W ICP, 250 W rf, 10BCl<sub>3</sub>/5Ar discharges (bottom).

at small source powers. As described below, the greater concentration of atomic F available at high source power contributed to thicker fluorinated surfaces, leading to the net deposition rather than etching.

Ion energy as well as ion flux and ion/neutral ratio is a strong variable affecting the etching. An example is shown for 10BCl<sub>3</sub>/5Ar discharges at 750 W ICP source power (Fig. 5). There was a rapid increase in etch rate of NiMnSb above

~250 V dc self-bias, indicative of the presence of a threshold ion energy for the etching of NiMnSb. Improved sputter desorption of etch products is also a likely contributor to the higher etch rates. Al<sub>2</sub>O<sub>3</sub> also showed an increase in etch rate under these conditions, due to the enhanced bond breaking with more energetic ions, and the etch rates saturated at higher ion energy. Selectivity changed from ~2 to ~9, depending on the ion energy.

NF<sub>3</sub>/Ar discharges did not provide high NiMnSb etch rates even at high dc self-bias. Only the addition of small (100 W) ICP source powers with either 5NF<sub>3</sub>/10Ar (Fig. 6, top) or 2NF<sub>3</sub>/13Ar (Fig. 6, bottom) showed etching as a function of dc self-bias. Increasing source power above 100 W produced deposition irrespective of ion energy applied. Moreover there was no etching of NiMnSb at high bias in 2NF<sub>3</sub>/13Ar, which might result from ion-assisted removal of the fluorine neutrals before they can react with the surface. This occurred at higher biases for higher NF<sub>3</sub> percentages.

In terms of surface roughness, Fig. 7 shows AFM images and root-mean-square (rms) surface roughness for NiMnSb etched with different gas compositions. It is apparent that surfaces etched with NF<sub>3</sub>/Ar discharges are quite smooth with rms values of 1.4–5.9 nm depending on gas composition (control samples have rms of 1.2–1.5 nm). By contrast, BCl<sub>3</sub>/Ar discharges produced much rougher surfaces with rms value of ~17 nm. This may be due to the nonstoichiometric surface resulting from different volatility of etch products. The rather spiky surface etched with 10BCl<sub>3</sub>/5Ar (Fig. 7, bottom right) reflects this assumption.

Turning to the near surface chemistry, surfaces etched with 5NF<sub>3</sub>/10Ar (Fig. 8, center) revealed Mn-enrichment with Sb-deficiency compared to the surface of unetched control (Fig. 8, top). We suspect that involatile Mn etch products contributed to forming MnO<sub>x</sub> upon exposure to the atmosphere after etching and the reaction layer on the surface prevented etching from proceeding even leading to the net deposition under most conditions.<sup>11</sup> On the contrary, 10BCl<sub>3</sub>/5Ar discharges produced a totally opposite result. Figure 8 (bottom) shows depth profile of NiMnSb in 750 W ICP, 250 W rf, 10BCl<sub>3</sub>/5Ar discharges. The surface has Sb enrichment with Mn deficiency, which indicates the formation of involatile chlorinated layer of Sb on the surface. We have previously found similar results with NF<sub>3</sub> etching of NiMnSb.<sup>11</sup>

#### IV. SUMMARY AND CONCLUSION

We have performed a parametric study of the etching of NiMnSb and Al<sub>2</sub>O<sub>3</sub>, based on BCl<sub>3</sub>/Ar, BCl<sub>3</sub>/H<sub>2</sub> and NF<sub>3</sub>/Ar chemistries in an inductively coupled plasma tool. Etching of NiMnSb showed a strong dependence on the gas composition, source power and dc self bias with BCl<sub>3</sub>/Ar. BCl<sub>3</sub>/H<sub>2</sub> discharges provided faster rates for NiMnSb, resulting from the HCl species created in these plasmas. Selectivities of NiMnSb over Al<sub>2</sub>O<sub>3</sub> were  $\geq 8$  in BCl<sub>3</sub>-based chemistry. By contrast NF<sub>3</sub>/Ar discharges had a rather narrow process window for the etching of NiMnSb. Nonoptimized conditions (either high source power or high percentage of NF<sub>3</sub>) led to the occurrence of net deposition rather than etching. This was in contrast to SF<sub>6</sub>-based etching, where etch rates  $> 1 \mu\text{m min}^{-1}$  were obtained, and deposition was not observed under any conditions.

#### ACKNOWLEDGMENTS

The work was partially supported by a DOD MURI monitored by the U. S. Air Force Office of Scientific Research (H. C. DeLong), Contract No. F49620-96-10026, a DARPA subcontract through Honeywell (ONR Grant No. N0001496-C-2114), and a DARPA subcontract through Florida State University (ONR Grant No. N00014-96-1-0767), the DARPA subcontracts both monitored by S. Wolf.

<sup>1</sup>See, for example, Phys. Today 48, 24 (1995); MRS Bull. 21, 17 (1996).

<sup>2</sup>C. Tsang, H. Santini, D. McCown, J. Lo, and R. Lee, IEEE Trans. Magn. 32, 7 (1996).

<sup>3</sup>See, for example, A. Fert and P. Bruno, in *Ultra-Thin Magnetic Structures II*, edited by B. Heinrich and J. A. C. Bland (Springer, Berlin, 1994).

<sup>4</sup>R. A. de Groot, F. M. Mueller, P. G. van Engen, and K. H. J. Buschow, Phys. Rev. Lett. 50, 2024 (1983).

<sup>5</sup>M. J. Otto, R. A. M. van Woerden, P. J. van der Valk, J. Wijngaard, C. F. van Bruggen, C. Hass, and K. S. H. Buschen, J. Phys.: Condens. Matter 1, 2341 (1989).

<sup>6</sup>J. A. Caballero, W. J. Geerts, F. Petroff, J. V. Thiele, D. Weller, and J. A. Childress, J. Magn. Magn. Mater. 177–181, 1229 (1998).

<sup>7</sup>J. A. Caballero, J. Petroff, Y. D. Park, A. Cabibbo, R. Morel, and J. R. Childress, J. Appl. Phys. 81, 2740 (1997).

<sup>8</sup>J. F. Bobo, P. R. Johnson, M. Kantzky, F. B. Mancoff, E. Tuncel, R. L. White, and B. M. Clenons, J. Appl. Phys. 81, 4164 (1997).

<sup>9</sup>J. S. Moodera, L. R. Kinder, J. M. Wong, and R. Meservey, Phys. Rev. Lett. 74, 8273 (1995).

<sup>10</sup>J. Hong, J. A. Caballero, W. J. Geerts, J. A. Childress, and S. J. Pearson, J. Electrochem. Soc. 144, 3602 (1997).

<sup>11</sup>J. Hong, J. A. Caballero, E. S. Lambers, J. R. Childress, and S. J. Pearson, J. Vac. Sci. Technol. A 16, 2153 (1998).

**THIS PAGE BLANK (USPTO)**